

Rothamsted Repository Download

A - Papers appearing in refereed journals

Nosrati, K. and Collins, A. L. 2019. Fingerprinting the contribution of quarrying to fine-grained bed. *River Research and Applications*. 35, pp. 290-300.

The publisher's version can be accessed at:

- <https://dx.doi.org/10.1002/rra.3408>

The output can be accessed at: <https://repository.rothamsted.ac.uk/item/8wq18>.

© 13 March 2019, Rothamsted Research. Licensed under the Creative Commons CC BY.

**Fingerprinting the contribution of quarrying to fine-grained
bed sediment in a mountainous catchment, Iran**

Journal:	<i>River Research and Applications</i>
Manuscript ID	RRA-18-0327.R1
Wiley - Manuscript type:	Research Article
Date Submitted by the Author:	n/a
Complete List of Authors:	Nosrati, Kazem; Shahid Beheshti University Faculty of Earth Sciences, Department of Physical Geography Collins, Adrian; Rothamsted Research - North Wyke, Sustainable Soils and Grassland Systems
Keywords:	Fingerprinting, quarrying, bed sediment, mountainous catchment, multiple statistical techniques

SCHOLARONE™
Manuscripts

1
2
3 1 **Fingerprinting the contribution of quarrying to fine-grained bed sediment in a**
4
5 2
6 **mountainous catchment, Iran**
7
8 3
9

10 4 Kazem Nosrati^{a,*}, Adrian L. Collins^b
11
12 5
13

14 6 *^aDepartment of Physical Geography, Faculty of Earth Sciences, Shahid Beheshti University,*

15
16
17 7 *1983969411 Tehran, Iran*

18
19 8 *^bSustainable Agriculture Sciences Department, Rothamsted Research, North Wyke,*

20
21 9 *Okehampton EX20 2SB, UK*
22
23
24 10

25
26 11 ***Corresponding author:**

27
28 12 **Kazem Nosrati**

29
30 13 Tel.: +98 21 29902604

31
32 14 Fax: +98 21 22431690

33
34 15 e-mail: k_nosrati@sbu.ac.ir
35
36
37 16
38
39

40 17 **Abstract**

41
42 18 **The contribution of quarrying in the context of multiple catchment sources of fine-**
43 **grained sediment has rarely been investigated.** This study assessed the relative importance of
44
45 19 quarrying as a sediment source alongside rangeland surface soils and channel banks in a
46
47 20 mountainous catchment in northern Tehran, Iran, using fingerprinting. Eight geochemical
48
49 21 tracers were measured on 24 potential sediment source samples and four fine-grained
50
51 22 sediment samples. Statistical analysis to select three different composite fingerprints for
52
53 23 discriminating the potential sediment sources comprised: (1) the Kruskal–Wallis H test (KW-
54
55 24 H), (2) a combination of KW-H and discriminant function analysis (DFA), and (3) a
56
57 25
58
59
60

1
2
3 26 combination of KW-H and principal components & classification analysis (PCCA). A
4
5 27 Bayesian un-mixing model was used to apportion sediment source contributions using the
6
7
8 28 three composite fingerprints. Using the KW-H composite signature, the respective relative
9
10 29 contributions (with uncertainty ranges) from channel banks, rangeland surface soils and
11
12 30 quarrying were estimated as 28.4% (10.9-46.8), 15.1% (6.6-22.7), and 56.6% (38.3-74.2),
13
14 31 compared to 35.4% (11.9-60.1), 13.4% (4.1-22.2) and 51.3% (26.5-74.3) using a composite
15
16 32 signature selected using a combination of KW-H and DFA, or 20.7% (3.9-41.7), 17.2% (4.4-
17
18 33 29.9) and 61.4% (44-78.8) using a fingerprint selected using KW-H and PCCA. The
19
20 34 different composite signatures therefore all consistently suggested that quarrying is the
21
22 35 dominant source of the fine-grained sediment samples. Potential mitigation measures
23
24 36 targeting this land use include closure to permit re-vegetation to reduce exposure of bare
25
26 37 surfaces to sediment mobilisation. Limitations and uncertainties associated with this
27
28 38 preliminary investigation are briefly discussed.

29
30
31
32
33 39 **Keywords:** Fingerprinting, quarrying, bed sediment, mountainous catchment, multiple
34
35 40 statistical techniques
36
37
38

39 41 40 42 **1. Introduction**

41
42 43 Anthropogenic geomorphology is defined as the discipline that embodies studying the
43
44 44 influence of human activities on earth surface forms and processes and thereby the landforms
45
46 45 shaped by weathering, erosion and particle transport (Li, Yang, Pu, & Liu, 2017). At least
47
48 46 one-third of the Earth's continental surface is affected by human activities acting as a
49
50 47 geomorphological agent that is equal in importance to other natural geomorphic factors in the
51
52 48 shaping of landforms (Rózsa, 2010). Such impacts have resulted in the use of the term
53
54 49 Anthropocene to refer to the current geological Epoch (Lewis & Maslin, 2015). The
55
56
57
58
59
60

1
2
3 50 geomorphic impact of humans is increasing and the identification and assessment of
4
5 51 unintended consequences will therefore be important.
6
7

8 52 One of the most important human impacts on some landscapes concerns quarrying.
9
10 53 Quarrying for the excavation of raw materials for construction in mountain settlements
11
12 54 generates a range of anthropogenic landforms including excavated, accumulated and
13
14 55 planation (anthropogenic features further modified by natural erosive processes) forms
15
16 56 (Dávid, 2010). Thus, land disturbance associated with quarrying generally increases erosion
17
18 57 and sediment yields and impacts on landscape sediment source patterns. In particular, surface
19
20 58 mining areas can accelerate natural soil erosion, which increases sediment loads in rivers
21
22 59 (Chalov, 2014; Chalov et al., 2015; Jaramillo, Baccard, Narinesingh, Gaskin, & Cooper,
23
24 60 2016; Pietroń, Chalov, Chalova, Alekseenko, & Jarsjö, 2017). Average accelerated soil
25
26 61 erosion rates in Iran have been estimated at 23 to 25 t ha⁻¹ year⁻¹ (Afshar, Ayoubi, & Jalalian,
27
28 62 2010; Karchegani, Ayoubi, Lu, & Honarju, 2011; Rahimi, Ayoubi, & Abdi, 2013), but,
29
30 63 importantly, the contribution of quarrying has not been determined.
31
32
33
34

35 64 Identifying the relative contributions of fine-grained (<63 µm) sediment from
36
37 65 quarrying can be used to help inform erosion mitigation strategies. Historically, different
38
39 66 techniques have been used to identify and apportion fine-grained sediment sources (Collins &
40
41 67 Walling, 2004). Sediment fingerprinting is a field based technique that apportions or un-
42
43 68 mixes, sampled target sediment into distinguishable sources through the use of different
44
45 69 natural and artificial tracers combined in a so-called composite fingerprint or signature.
46
47 70 Comprehensive recent literature reviews (e. g. Collins et al., 2017; Owens et al., 2017) reveal
48
49 71 that the fingerprinting approach has not been used to investigate fine-grained sediment
50
51 72 contributions from quarrying in mountainous environments. Accordingly, the main objective
52
53 73 of this study was to use a composite fingerprinting procedure combining geochemical tracers
54
55 74 and different statistical tests for source discrimination with a Bayesian un-mixing model for
56
57
58
59
60

1
2
3 75 source apportionment, to determine the relative importance of quarrying in a small sub-
4
5 76 catchment of the Farahzad drainage basin, northern Tehran, Iran. It was hypothesized that
6
7 77 quarrying is the primary fine-grained sediment source in the study catchment. **Different**
8
9 78 **statistical tests provide a basis for exploring uncertainties in source apportionment provided**
10
11 79 **by alternative composite signatures.**
12
13
14
15
16
17

18 81 **2. Materials and methods**

19 20 82 **2.1. Study catchment**

21
22 83 The study area is a sub-catchment (77.4 ha) of the Farahzad (Younjeh-Zar) drainage
23
24 84 basin and is located to the north of the capital city of Iran, Tehran city, located between 51°
25
26 85 $19' 32''\text{E}$ to $51^{\circ} 20' 15''\text{E}$ longitude and $35^{\circ} 47' 50''\text{N}$ to $35^{\circ} 48' 30''\text{N}$ latitude in the Southern
27
28 86 Alborz Mountains (Figure 1; S1). Land cover comprises 72% grazing land (55.8 ha), 12%
29
30 87 orchard (9.5 ha), and 15% quarrying (11.8 ha). **The catchment lithology comprises middle**
31
32 88 **Eocene massive green tuff and shale with basic lava flows (E^{tsv}).** Mean annual discharge at
33
34 89 the outlet of the Farahzad drainage basin, based on regional analysis, is $0.37 \text{ m}^3 \text{ s}^{-1}$. The
35
36 90 annual average suspended and bed sediment loads, **based on regional analysis of data**
37
38 91 **collected at eight gauges,** are 10646 t yr^{-1} and 2661 t yr^{-1} , respectively.
39
40
41
42

43 92 Figure 1

44
45 93 Mining in the study area comprises stone (green tuff stone) quarrying for excavating
46
47 94 raw materials for buildings, recreational complexes (parks), and ornamental stones. The
48
49 95 quarrying in the study area has been active for ca. 25 years. At least 10,000 ton yr^{-1} are
50
51 96 extracted from the main mine. Quarry walls and floors, talus slopes, rainwater grooves and
52
53 97 debris aprons are visible at the main mine.
54
55
56
57
58
59
60

99 2.2. Catchment sampling and laboratory measurements

100 *Sediment source sampling:* Prior to sampling, field surveys were undertaken to identify
101 potential sediment sources across the study area and these were classified on the basis of soil
102 erosion types: quarrying, rangeland surface soil erosion and subsurface erosion of stream
103 channel banks. A total of 24 source samples were collected to represent these key potential
104 sediment sources, comprising eight samples from each of the three source types. In order to
105 increase the representativeness of the individual source samples, each surface sample for
106 quarrying (i.e. the excavated bed or disposal surface) or the rangeland, comprised a
107 composite of five sub-samples collected within ca. 40 m² at a specific site, whereas each
108 subsoil sample from eroding channel banks or quarry walls comprised a composite of 10 sub-
109 samples collected within a ~20 m long reach (interval 2 m) at each sampling site. Surface
110 erosion source samples were collected from the upper 5 cm of the soil layer (Nosrati, 2017).
111 Channel bank samples were collected by scraping material from the full vertical extent of
112 actively eroding profiles (Nosrati, Govers, Semmens, & Ward, 2014).

113 *Fine-grained sediment sampling:* Samples of fine-grained sediment deposited on the river
114 bed were collected at the overall outlet of the study catchment (Figure 1). The focus here was
115 on samples of the 'drape' material that appeared to have been recently deposited (i.e. no
116 vegetation/macrophyte cover; (e. g. Collins & Walling, 2007). Successful use of such
117 deposits has previously been reported in Iran to fingerprint sediment in a region with poor
118 site access (Nosrati, 2017; Nosrati, Collins, & Madankan, 2018). In order to ensure that the
119 sediment samples were as representative as labour and financial resources permitted, 10 sub-
120 samples were collected at each of four channel sampling sites along a ~20 m reach (interval 2
121 m) and combined into four individual composite samples. All source and sediment samples
122 were retrieved from the field between April 4th and April 10th 2017 after a continuous rainfall
123 period.

1
2
3 124
4
5 125 *Laboratory analyses:* Any sediment source tracing study needs to make careful decisions
6
7 126 about the particle size fraction used, since this decision can impact heavily on the
8
9 127 comparability of source and sediment samples and the reliability of the apportionment results
10
11 128 generated (Collins et al., 2017; Laceby et al., 2017). Dry sieving (using sieve apertures of 500
12
13 129 μm , 300 μm , 250 μm , 212 μm , 125 μm , 75 μm and 63 μm) revealed that the <63 μm fraction was
14
15 130 the dominant fraction of the ‘drape’ sediment samples. Consequently, only the <63 μm
16
17 131 fraction of the target sediment and source samples was used for the analysis and comparison
18
19 132 of fingerprint properties. In order to measure the geochemistry (elements selected *a priori* on
20
21 133 the basis of previous experience) of samples (S2), one gram (<63 μm) of the sediment and
22
23 134 source samples was digested for two hours at 95 °C in aqua regia (HCl–HNO₃; 3:1) using a
24
25 135 Velp Thermo-reactor. Extracts were filtered through S&S ME24 (0.2 μm) filter papers and
26
27 136 the solutions analysed by a Varian SpectrAA-20 Plus calibrated using an element standard
28
29 137 solution (Merck KGaA, Frankfurter, Germany) for Ca, Fe, K, Mg, Mn, Na, and Ni
30
31 138 concentrations. Analytical errors were <5%. Total organic carbon (TOC) content was
32
33 139 measured by the Walkley-Black method (Skjemstad & Baldock, 2008).
34
35
36
37
38
39
40
41

42 141 **2.3. Selection of composite signatures for discriminating the potential fine-grained** 43 44 142 **sediment sources**

45
46 143 A three-part procedure was used to assess tracer conservation. Firstly, a standard
47
48 144 bracket or range test (Foster & Lees, 2000) was used to identify non-conservative tracers.
49
50 145 Secondly, the tracers were screened using a stricter test whereby the sediment sample means
51
52 146 should fall within the corresponding source means rather than their full ranges (Wilkinson,
53
54 147 Hancock, Bartley, Hawdon, & Keen, 2013). Thirdly, biplots of tracers included in the final
55
56
57
58
59
60

1
2
3 148 statistically-verified composite fingerprints were also used to compare source and sediment
4
5 149 samples (Collins et al., 2017).

6
7
8 150 Statistical analysis (STATISTICA V.8.0; (StatSoft, 2008) for identifying three
9
10 151 different composite fingerprints for discriminating between the potential sediment sources
11
12 152 used three approaches (Nosrati et al., 2018): the Kruskal-Wallis H-test (KW-H); KW-H
13
14 153 combined with discriminant function analysis (DFA); and KW-H combined with principal
15
16
17 154 component and classification analysis (PCCA).

18
19 155

20 21 156 **2.4. Source apportionment**

22
23
24 157 The Modified MixSIR model (Nosrati et al., 2018; Nosrati et al., 2014) provides a
25
26 158 Bayesian (e. g. Cooper, Krueger, Hiscock, & Rawlins, 2014; Massoudieh, Gellis, Banks, &
27
28 159 Wiczorek, 2013) rather than frequentist approach (Collins, Walling, & Leeks, 1997) to
29
30 160 apportionment modelling.

31
32
33 161 Modified MixSIR (S3) estimates source apportionment as probability distributions for
34
35 162 the relative contribution of each source to target sediment samples using: 1) determination of
36
37 163 the prior probability distributions, 2) generation of a likelihood function, and 3) generation of
38
39 164 posterior probability distributions to adjust the priors.

40
41
42 165 10^6 samples were drawn from the posterior distribution of the estimated target sediment
43
44 166 mixtures in MATLAB. The model predictions of source proportions were evaluated using a
45
46 167 small set of virtual sediment mixtures (Collins et al., 2017; Leticia Palazón et al., 2015) for
47
48 168 each composite signature. Here, three virtual sediment mixtures were constructed using a
49
50 169 range of source proportions: equal proportions from all sources; 90% quarrying, 5%
51
52 170 rangeland surface soils, 5% channel banks, and; 5% quarrying, 75% rangeland surface soils
53
54 171 and 20% channel banks. Since the virtual sediment mixtures were constructed using the
55
56 172 measured tracer data for the source samples, the tracer concentrations in the virtual mixtures

173 satisfied the bracket test for tracer conservation. The accuracy of the modelling in solving the
 174 virtual sediment mixtures was assessed using the averaged root mean square error (RMSE)
 175 and mean absolute error between the predicted ($Y_{\text{Predicted}}$) and known (Y_{Known}) source
 176 proportions using each final composite signature (Eqs. 1 and 2):

$$177 \quad RMSE = \sqrt{\frac{\sum_{i=1}^n (Y_{\text{Known}} - Y_{\text{Predicted}})^2}{n}} \quad \text{Eq. 1}$$

$$178 \quad MAE = \frac{\sum_{i=1}^n |Y_{\text{Known}} - Y_{\text{Predicted}}|}{n} \quad \text{Eq. 2}$$

180 3. Results and discussion

181 3.1. Composite fingerprints for discriminating the potential sediment sources

182 Table 1 presents the tracer concentrations in the samples. In addition, Table 1 presents
 183 the results of normality tests showing that all tracers exhibited normal distributions ($p > 0.05$)
 184 (a prerequisite for using the tracers in a Bayesian un-mixing model). The results of the
 185 standard bracket test suggested that all tracers were generally conservative in terms of their
 186 concentrations, despite the potential risk of change during sediment mobilisation, transport
 187 and delivery. In addition, the results of comparing the sediment means with the
 188 corresponding source means likewise suggested that all tracers were conservative following
 189 mobilisation and delivery to, and through, the channel system (Table 1). Here, it is important
 190 to remember that the range tests provide a simple mathematical means of assessing whether
 191 processes such as dissolution, adsorption and precipitation have substantially altered the
 192 concentrations of the sediment tracers in comparison with those of the sources. These
 193 mathematical tests do not provide definitive evidence that non-conservative behaviour is
 194 totally absent. Table 1 also presents the results of applying the KW-H test which indicated

1
2
3 195 that six tracers (Ca, Fe, Mg, Mn, Ni and TOC) exhibited a statistically significant difference
4
5 196 ($p \leq 0.05$) between the three potential sediment sources. Those tracers (K and Na) unable to
6
7 197 discriminate the potential sources using KW-H were discarded from further analysis.
8
9

10 198 Table 1
11

12 199 The six tracers selected by the KW-H test were used in stepwise DFA (Table 2). The
13
14 200 largest eigenvalue of the first function (12.6) corresponds to the eigenvector in the direction
15
16 201 of the maximum spread of the groups' means. The Wilk's lambda value of the first function
17
18 202 (0.019) suggested that 98.1% of the total variance among the potential sediment sources was
19
20 203 explained by these tracers. The canonical correlation value was 0.96, revealing a strong
21
22 204 correlation between the discriminant scores and individual sources.
23
24

25 205 The squared Mahalanobis distance showed that the sediment sources were
26
27 206 distinguished by the shortlisted tracers (Table 2), with the greatest differences being between
28
29 207 channel banks and rangeland surface soils (57.6) and rangeland surface soils and quarrying
30
31 208 (49.6). For channel banks and quarrying, the squared Mahalanobis distance was the least
32
33 209 (14.4). The forward stepwise DFA yielded classification matrices assigning 95.8% of the
34
35 210 cases (i.e., source samples) to the correct groups (Table 2). Stepwise selection using Wilks'
36
37 211 lambda generated a composite signature comprising four tracers (Ca, Fe, Mn and Ni) which
38
39 212 provided significant discriminatory power on the basis of the DFA model (Table 3). The
40
41 213 results of different tests within DFA indicated that the discriminatory power of Mn is perfect
42
43 214 (Table 3). Here, Partial Wilks' lambda is the Wilks' lambda for the unique contribution of the
44
45 215 respective tracer to the discrimination between individual sediment source groups. The
46
47 216 smaller the Partial Wilks' lambda, the greater the contribution to the overall discrimination
48
49 217 provided by the composite fingerprint. In this case, the Partial Wilks' lambda values
50
51 218 suggested that Mn contributed the most, Ni second most, Ca third most and Fe the least to the
52
53 219 overall discrimination (Table 3). A scatterplot using the first and second discriminant
54
55
56
57
58
59
60

1
2
3 220 functions calculated using backward DFA confirmed that the samples collected to
4
5 221 characterise the different potential sediment sources were well separated (Figure 2).

6
7
8 222 Table 2

9
10 223 Table 3

11
12 224 Figure 2

13
14
15 225 Tracers selected by the KW-H test (Ca, Fe, Mg, Mn, Ni and TOC) were also entered
16
17 226 into PCCA to help reduce the number of tracers and multicollinearity. The results of a scree
18
19 227 plot (Figure 3a) showed that the first three principal components (PCs) yielded the most
20
21 228 interpretable factor pattern (Table 4). These three PCs accounted for >88% of the variability
22
23 229 among the tracer values for the three source groups (Table 4). The highly-weighted tracers
24
25 230 under PC1 with absolute values within 10% of the highest tracer (0.90 value for TOC)
26
27 231 loading (the loading of selected tracers should be larger than 0.81) were Fe, Mn and Ni. Only
28
29 232 TOC was retained for the final composite signature because these four tracers were strongly
30
31 233 correlated ($r > 0.60$). Under PC2, the Mg was the highest tracer with a loading value of 0.79.
32
33 234 In this case, the loading of selected tracers should exceed 0.71, but all loading values were
34
35 235 less than this threshold and therefore only Mg was retained for the final composite signature.
36
37 236 Under PC3, the highly-weighted tracer (0.66 value for Ca) with an absolute value within 10%
38
39 237 of the highest tracer loading (the loading of selected tracers should be larger than 0.59) was
40
41 238 Ca (Table 4). Accordingly, these results selected three tracers (TOC, Mg and Ca) as an
42
43 239 alternative composite fingerprint on the basis of the PCCA model. Projection of the cases on
44
45 240 the PC-plane using PCCA (Figure 3b) confirmed that the set of selected tracers (i.e.
46
47 241 composite fingerprint) clearly provided good discrimination between the three potential
48
49 242 sediment sources.

50
51
52 243 Figure 3

53
54
55 244 Table 4

1
2
3 245 PCs scores were also calculated using the resulting component score coefficient
4
5 246 matrix and tested for significant differences between the potential sediment sources using
6
7 247 one-way ANOVA (F-test) and Tukey HSD post-hoc tests ($p \leq 0.05$) (Table 4). PC scores for
8
9 248 all three PCs varied significantly with sediment sources (Table 4). Thus, the tracers related to
10
11 249 these PCs provided a basis for selection of a third alternative composite signature (TOC, Mg
12
13 250 and Ca).
14

15
16
17 251 For the tracers selected in the three final composite signatures, the biplots of all tracer
18
19 252 pairings for source and sediment samples were compared as part three of the screening for
20
21 253 conservative behaviour. The results confirmed that there was no major tracer transformation
22
23 254 during sediment mobilisation and delivery (Figure 4). **Of the final tracers selected, TOC has**
24
25 **the potential to be influenced by instream productivity. The dataset assembled for this study,**
26
27 **however, was subjected to three tests for tracer non-conservative behaviour (basic and stricter**
28
29 **range tests, biplots). Since TOC passed all three tests, significant transformation was not**
30
31 **deemed to be present on the basis of the sediment sampling location used.**
32
33
34

35 259 Figure 4
36
37
38 260

39 40 261 **3.2. Sediment source contributions**

41
42 262 Model runs converged on the posterior contributions from the sources using each of
43
44 263 the three different composite signatures selected using the statistical tests (Figure 5). Using
45
46 264 the composite fingerprint selected by KW-H, relative contributions (with corresponding
47
48 265 uncertainty ranges) from channel banks, rangeland surface soils and quarrying were estimated
49
50 266 as 28.4% (10.9-46.8), 15.1% (6.6-22.7), and 56.6% (38.3-74.2), respectively. Using the KW-
51
52 267 H and DFA signature, the corresponding respective contributions and associated uncertainty
53
54 268 ranges were predicted as 35.4% (11.9-60.1), 13.4% (4.1-22.2) and 51.3% (26.5-74.3).
55
56 269 Finally, on the basis of the KW-H and PCCA signature, the relative contributions from
57
58
59
60

1
2
3 270 channel banks, rangeland surface soils and quarrying were computed as 20.7% (3.9-41.7),
4
5 271 17.2% (4.4-29.9) and 61.4% (44-78.8), respectively. Root mean square differences between
6
7 272 the estimated sediment contributions from channel banks, rangeland surface soils and
8
9 273 quarrying using the three different composite signatures were estimated as 10.4%, 2.7% and
10
11 274 7.1%, respectively. Source contributions were therefore sensitive to the signature used,
12
13 275 underscoring the need to use multiple fingerprints when investigating sediment source
14
15 276 contributions (cf. Collins et al., 2017; Nosrati et al., 2018; Owens et al., 2017; L. Palazón &
16
17 277 Navas, 2017). Here, it is more informative to use a combination of different statistical tests
18
19 278 rather than selecting alternative composite signatures using the same test, since application of
20
21 279 more than one test ensures additional dimensionality in the tracer assessment.
22
23
24
25

26 280 Figure 5

27
28 281 Comparison of the predicted and known relative contributions from channel banks,
29
30 282 rangeland surface soils and quarrying using the three different composite signatures and the
31
32 283 virtual sediment mixtures showed that the RMSE and MAE ranged between 0.3% to 20.9%
33
34 284 and 0.3% to 18.9%, respectively (Table 5). The overall average RMSE and MAE for the
35
36 285 modelled source predictions using the virtual mixtures were 12.1% and 8.3%, respectively
37
38 286 (Table 5). These error levels were judged to be acceptable.
39
40
41

42 287 Table 5

43
44 288 The different composite signatures all suggested that quarrying was the dominant
45
46 289 source of the fine-grained sediment samples. Using the areas of rangeland surface soils,
47
48 290 quarrying and channel banks (52, 11.8 and 3.8 ha, respectively) the respective specific
49
50 291 importance (based on the overall mean relative contributions from the three composite
51
52 292 fingerprints) of these sources was estimated as 0.3, 4.8 and 7.4. Here, the quarrying and
53
54 293 channel bank areas are small and so the high specific contributions indicate much higher
55
56 294 erosion and sediment delivery rates for these sources. Recent studies in other areas of the
57
58
59
60

1
2
3 295 world have also revealed the impact of mining and quarrying on sediment dynamics. Pietroní
4
5 296 et al. (2017), for example, concluded that patterns of increased sediment load along the Tuul
6
7 297 River that runs through the Zaamar Goldfield in Mongolia is consistent with soil loss being
8
9 298 two to three orders of magnitude higher in mining areas than in the surrounding natural areas
10
11 299 dominated by grasslands. The same authors also reported that the sediment load contribution
12
13 300 from mining areas was insensitive to changes in hydrometeorological conditions. Likewise,
14
15 301 Jaramillo et al. (2016) reported that a limestone quarry in the Don Juan River sub-catchment
16
17 302 of the Maracas-Saint Joseph River catchment (MSJRC) located in Trinidad, is the largest
18
19 303 producer of suspended and bed sediment in terms of soil loss per unit area. Chalov (2014)
20
21 304 estimated the total sediment delivery from opencast placer mining located in the north of
22
23 305 Russia's Kamchatka Peninsula is 60 t yr^{-1} which is three orders of magnitude higher than
24
25 306 from non-mined streams. Chalov et al. (2015) highlighted mining areas as important
26
27 307 contributors to sediment fluxes in the Selenga River basin, draining areas of Russia and
28
29 308 Mongolia. Our findings are therefore consistent with other studies; quarrying can be a major
30
31 309 fine-grained sediment source.
32
33
34
35
36
37
38
39

311 3.3 Limitations

312 The sediment source fingerprinting study reported here inevitably has some inherent
313 limitations and uncertainties. Some of these are associated with either available resources or
314 the challenges of working in a mountainous environment, but others remain common to
315 source tracing work more generally. Limited numbers of source and sediment samples were
316 collected and although the sampling strategy was not probability based, nor are those
317 strategies reported by most studies in the existing international literature (Collins et al.,
318 2017). Since the target bed sediment samples were collected from the study catchment outlet
319 only, rather than at a number of locations along the channel network, the estimated source
320

1
2
3 320 proportions should be interpreted as scale dependent. Clearly, in steep mountainous terrain, it
4
5 321 is very challenging to sample multiple channel locations, but it is also noteworthy that many
6
7 322 existing published studies suffer from this limitation regardless of the study environment and
8
9 323 any potential fieldwork challenges (Collins et al., 2017). Specifically, in the case of this
10
11 324 study, it would be useful to sample sediment upstream and downstream of the quarrying to
12
13 325 explore the evolution of the sediment signatures and the corresponding source proportions.
14
15 326 Target sediment sampling focused on surface drape bed sediment rather than suspended
16
17 327 sediment samples and it is useful to bear in mind that source ascription can differ for different
18
19 328 sediment types (e. g. channel bed versus suspended sediment) as a result of erosion process
20
21 329 dynamics (Nicholls, 2000). Clearly, the sediment sampling needs to be extended to improve
22
23 330 the temporal representativeness of the dataset and here the findings presented in this paper
24
25 331 should be interpreted as preliminary and providing confirmation that the fingerprinting
26
27 332 approach works in the study area. Differing transport characteristics of mobilised
28
29 333 minerogenic and organic fractions of source material require more explicit consideration in
30
31 334 the context of the tracers combined in final composite signatures. The preliminary source
32
33 335 estimates underscore the importance of quarrying, but these results need to be confirmed by
34
35 336 extending the sampling both spatially (i.e. more channel locations) and temporally (i.e. more
36
37 337 storms). The Modified MixSIR model uses Bayesian as opposed to frequentist distribution-
38
39 338 based principles and predicted source proportions can be biased by the choice of sediment un-
40
41 339 mixing model structure (Lacey & Olley, 2015; Smith & Blake, 2014). Previous work has
42
43 340 explored a range of weightings including those for tracer analytical precision (Collins et al.,
44
45 341 1997) or discriminatory power (e. g. Collins et al., 2014) and spatial variations in tracers by
46
47 342 source category (e. g. Gellis & Noe, 2013; Wilkinson et al., 2013) as well as corrections for
48
49 343 particle size (Collins et al., 1997) or organic matter (e. g. Gellis & Noe, 2013) selectivity.
50
51 344 Here, given the inherent uncertainties associated with these numerical model parameters
52
53
54
55
56
57
58
59
60

1
2
3 345 (Koiter, Owens, Petticrew, & Lobb, 2018; Laceby et al., 2017), such additions to un-mixing
4
5 346 model structure were avoided. The predictions for source apportionment generated by
6
7 347 Modified MixSIR were not evaluated using artificial mixtures (Brosinsky, Foerster, Segl, &
8
9 348 Kaufmann, 2014) of known source material proportions. Instead, virtual mixtures were
10
11 349 constructed from the measured data on the sediment samples. Where possible, it is preferable
12
13 350 to use artificial mixtures by mixing real source samples to better represent any potential
14
15 351 effects of grain size contrasts between the individual source groups in the study catchment.
16
17 352 **The source discrimination and apportionment relied on statistically-verified solutions, but it**
18
19 353 **remains important to consider the physico-chemical basis for tracer utility in fingerprinting**
20
21 354 **studies. Where access to facilities and resources permit, it is meaningful to explore the**
22
23 355 **corresponding estimates provided by alternative tracer property types as a means of testing**
24
25 356 **consistency in predictions.**
26
27
28
29
30
31
32
33

34 358 **4. Conclusion**

35
36 359 Further research is needed to corroborate the preliminary findings here using
37
38 360 extended (spatially along the channel network and temporally) sediment sampling and testing
39
40 361 additional types of tracers with the potential to discriminate between different surface and
41
42 362 subsurface sediment sources. Future management activities to reduce suspended and bed
43
44 363 sediment loads, not only from the study catchment but also from others with similar land use
45
46 364 issues, should focus on improving the regulation and management of quarrying operations.
47
48 365 Here, it remains important to compile evidence on the efficacy of sediment control options as
49
50 366 such information will in itself, assist uptake by stakeholders.
51
52
53
54
55
56

57 368 **Acknowledgements:** This project was funded by a grant (grant number 600.1197) from the
58
59 369 research council of Shahid Beheshti University, Tehran, Iran. ALC was supported by
60

1
2
3 370 strategic funding from the UK Biotechnology and Biological Sciences Research Council
4
5 371 (BBSRC grant BBS/E/C/000I0330).
6
7

8 372

9
10 373 **References**

11
12 374 Afshar, F. A., Ayoubi, S., & Jalalian, A. (2010). Soil redistribution rate and its relationship
13
14 375 with soil organic carbon and total nitrogen using ^{137}Cs technique in a cultivated
15
16 376 complex hillslope in western Iran. *Journal of environmental radioactivity*, 101(8),
17
18
19 377 606-614.

20
21 378 Brosinsky, A., Foerster, S., Segl, K., & Kaufmann, H. (2014). Spectral fingerprinting:
22
23 379 sediment source discrimination and contribution modelling of artificial mixtures
24
25 380 based on VNIR-SWIR spectral properties. *Journal of soils and sediments*, 14(12),
26
27
28 381 1949-1964.

29
30 382 Chalov, S. R. (2014). Effects of placer mining on suspended sediment budget: case study of
31
32 383 north of Russia's Kamchatka Peninsula. *Hydrological Sciences Journal*, 59(5), 1081-
33
34 384 1094.

35
36
37 385 Chalov, S. R., Jarsjö, J., Kasimov, N. S., Romanchenko, A. O., Pietroń, J., Thorslund, J., &
38
39 386 Promakhova, E. V. (2015). Spatio-temporal variation of sediment transport in the
40
41 387 Selenga River Basin, Mongolia and Russia. *Environmental Earth Sciences*, 73(2),
42
43
44 388 663-680.

45
46 389 Collins, A., Pulley, S., Foster, I. D., Gellis, A., Porto, P., & Horowitz, A. (2017). Sediment
47
48 390 source fingerprinting as an aid to catchment management: a review of the current state
49
50 391 of knowledge and a methodological decision-tree for end-users. *Journal of*
51
52 392 *Environmental Management*, 194, 86-108.
53
54
55
56
57
58
59
60

- 1
2
3 393 Collins, A., & Walling, D. (2004). Documenting catchment suspended sediment sources:
4
5 394 problems, approaches and prospects. *Progress in Physical Geography*, 28(2), 159-
6
7 395 196.
8
9
10 396 Collins, A., & Walling, D. (2007). Sources of fine sediment recovered from the channel bed
11
12 397 of lowland groundwater-fed catchments in the UK. *Geomorphology*, 88(1-2), 120-
13
14 398 138.
15
16
17 399 Collins, A., Walling, D., & Leeks, G. (1997). Sediment sources in the Upper Severn
18
19 400 catchment: a fingerprinting approach. *Hydrology and Earth System Sciences*
20
21 401 *Discussions*, 1(3), 509-521.
22
23
24 402 Collins, A., Williams, L., Zhang, Y., Marius, M., Dungait, J., Smallman, D., . . . Jones, J.
25
26 403 (2014). Sources of sediment-bound organic matter infiltrating spawning gravels
27
28 404 during the incubation and emergence life stages of salmonids. *Agriculture,*
29
30 405 *Ecosystems & Environment*, 196, 76-93.
31
32
33 406 Cooper, R. J., Krueger, T., Hiscock, K. M., & Rawlins, B. G. (2014). Sensitivity of fluvial
34
35 407 sediment source apportionment to mixing model assumptions: a Bayesian model
36
37 408 comparison. *Water resources research*, 50(11), 9031-9047.
38
39
40 409 Dávid, L. (2010). Quarrying and other minerals. In J. Szabó, L. Dávid, & D. Lóczy (Eds.),
41
42 410 *Anthropogenic Geomorphology: A Guide to Man-Made Landforms* (pp. 113-130):
43
44 411 Springer.
45
46
47 412 Foster, I. D., & Lees, J. A. (2000). Tracers in Geomorphology: theory and applications in
48
49 413 tracing fine particulate sediments. In I. I. D. Foster (Ed.), *Tracers in gemorphology*
50
51 414 (pp. 3-20). Chichester: J. Wiley & Sons.
52
53
54 415 Gellis, A. C., & Noe, G. B. (2013). Sediment source analysis in the Linganore Creek
55
56 416 watershed, Maryland, USA, using the sediment fingerprinting approach: 2008 to
57
58 417 2010. *Journal of soils and sediments*, 13(10), 1735-1753.
59
60

- 1
2
3 418 Jaramillo, F., Baccard, M., Narinesingh, P., Gaskin, S., & Cooper, V. (2016). Assessing the
4
5 419 role of a limestone quarry as sediment source in a developing tropical catchment.
6
7 420 *Land Degradation & Development*, 27(4), 1064-1074.
8
9
10 421 Karchegani, P. M., Ayoubi, S., Lu, S. G., & Honarju, N. (2011). Use of magnetic measures to
11
12 422 assess soil redistribution following deforestation in hilly region. *Journal of Applied*
13
14 423 *Geophysics*, 75(2), 227-236.
15
16
17 424 Koiter, A. J., Owens, P. N., Petticrew, E. L., & Lobb, D. A. (2018). Assessment of particle
18
19 425 size and organic matter correction factors in sediment source fingerprinting
20
21 426 investigations: An example of two contrasting watersheds in Canada. *Geoderma*, 325,
22
23 427 195-207.
24
25
26 428 Laceby, J. P., Evrard, O., Smith, H. G., Blake, W. H., Olley, J. M., Minella, J. P., & Owens,
27
28 429 P. N. (2017). The challenges and opportunities of addressing particle size effects in
29
30 430 sediment source fingerprinting: a review. *Earth-Science Reviews*, 169, 85-103.
31
32
33 431 Laceby, J. P., & Olley, J. (2015). An examination of geochemical modelling approaches to
34
35 432 tracing sediment sources incorporating distribution mixing and elemental correlations.
36
37 433 *Hydrological Processes*, 29(6), 1669-1685.
38
39
40 434 **Lewis, S. L., & Maslin, M. A. (2015). Defining the anthropocene. *Nature*, 519(7542), 171.**
41
42 435 Li, J., Yang, L., Pu, R., & Liu, Y. (2017). A review on anthropogenic geomorphology.
43
44 436 *Journal of Geographical Sciences*, 27(1), 109-128.
45
46
47 437 Massoudieh, A., Gellis, A., Banks, W. S., & Wieczorek, M. E. (2013). Suspended sediment
48
49 438 source apportionment in Chesapeake Bay watershed using Bayesian chemical mass
50
51 439 balance receptor modeling. *Hydrological Processes*, 27(24), 3363-3374.
52
53
54 440 **Nicholls, D. J. (2000). *The source and behaviour of fine sediment deposits in the river***
55
56 441 ***Torridge, Devon and their implications for salmon spawning*. University of Exeter,**
57
58
59
60

- 1
2
3 442 Nosrati, K. (2017). Ascribing soil erosion of hillslope components to river sediment yield.
4
5 443 *Journal of Environmental Management*, 194, 63-72.
6
7
8 444 Nosrati, K., Collins, A. L., & Madankan, M. (2018). Fingerprinting sub-basin spatial
9
10 445 sediment sources using different multivariate statistical techniques and the Modified
11
12 446 MixSIR model. *Catena*, 164, 32-43.
13
14
15 447 Nosrati, K., Govers, G., Semmens, B. X., & Ward, E. J. (2014). A mixing model to
16
17 448 incorporate uncertainty in sediment fingerprinting. *Geoderma*, 217, 173-180.
18
19
20 449 Owens, P., Blake, W., Gaspar, L., Gateuille, D., Koiter, A., Lobb, D., . . . Woodward, J.
21
22 450 (2017). Fingerprinting and tracing the sources of soils and sediments: Earth and ocean
23
24 451 science, geoarchaeological, forensic, and human health applications. *Earth-Science*
25
26 452 *Reviews*, 162, 1-23.
27
28
29 453 Palazón, L., Latorre, B., Gaspar, L., Blake, W. H., Smith, H. G., & Navas, A. (2015).
30
31 454 Comparing catchment sediment fingerprinting procedures using an auto-evaluation
32
33 455 approach with virtual sample mixtures. *Science of the Total Environment*, 532, 456-
34
35 456 466.
36
37
38 457 Palazón, L., & Navas, A. (2017). Variability in source sediment contributions by applying
39
40 458 different statistic test for a Pyrenean catchment. *Journal of Environmental*
41
42 459 *Management*, 194, 42-53. doi:<https://doi.org/10.1016/j.jenvman.2016.07.058>
43
44
45 460 Pietroń, J., Chalov, S. R., Chalova, A. S., Alekseenko, A. V., & Jarsjö, J. (2017). Extreme
46
47 461 spatial variability in riverine sediment load inputs due to soil loss in surface mining
48
49 462 areas of the Lake Baikal basin. *Catena*, 152, 82-93.
50
51
52 463 Rahimi, M. R., Ayoubi, S., & Abdi, M. R. (2013). Magnetic susceptibility and Cs-137
53
54 464 inventory variability as influenced by land use change and slope positions in a hilly,
55
56 465 semiarid region of west-central Iran. *Journal of Applied Geophysics*, 89, 68-75.
57
58
59
60

- 1
2
3 466 Rózsa, P. (2010). Nature and extent of human geomorphological impact—a review. In J.
4
5 467 Szabó, L. Dávid, & D. Lóczy (Eds.), *Anthropogenic Geomorphology: A Guide to*
6
7 468 *Man-Made Landforms* (pp. 273-291): Springer.
- 8
9
10 469 Skjemstad, J. O., & Baldock, J. A. (2008). Total and organic carbon. In M. R. Carter & E. G.
11
12 470 Gregorich (Eds.), *Soil Sampling and Methods of Analysis* (2 ed., pp. 225-237). Boca
13
14 471 Raton: CRC Press, Taylor & Francis Group.
- 15
16
17 472 Smith, H. G., & Blake, W. H. (2014). Sediment fingerprinting in agricultural catchments: a
18
19 473 critical re-examination of source discrimination and data corrections. *Geomorphology*,
20
21 474 *204*, 177-191.
- 22
23
24 475 StatSoft. (2008). STATISTICA: [data analysis software system], Version 8.0 for Windows
25
26 476 update. StatSoft, Inc. (Version 8.0 for Windows update).
- 27
28 477 Wilkinson, S. N., Hancock, G. J., Bartley, R., Hawdon, A. A., & Keen, R. J. (2013). Using
29
30 478 sediment tracing to assess processes and spatial patterns of erosion in grazed
31
32 479 rangelands, Burdekin River basin, Australia. *Agriculture, Ecosystems & Environment*,
33
34 480 *180*, 90-102.
- 35
36
37
38 481

Table 1

Tracer concentration data for the source and fine-grained sediment samples, results of the Kolmogorov-Smirnov test for normality, and Kruskal-Wallis H-test results for sediment source discrimination.

Sediment sources		Tracers							
		Ca (mg kg ⁻¹)	Fe (mg kg ⁻¹)	K (mg kg ⁻¹)	Mg (mg kg ⁻¹)	Mn (mg kg ⁻¹)	Na (mg kg ⁻¹)	Ni (mg kg ⁻¹)	TOC (g kg ⁻¹)
Channel banks	Mean	23125.0	15625.0	13433.5	26713.6	669.1	1873.4	112.2	4.8
	SD	10870.9	2754.4	2354.0	10585.7	133.1	492.5	25.9	2.8
Rangeland surface soils	Mean	14687.5	29050.5	14652.1	23489.0	1383.3	1606.2	52.4	13.4
	SD	5560.6	2881.5	3493.2	3071.5	135.7	218.1	17.3	2.3
Quarrying	Mean	45044.6	19116.2	15807.6	31816.7	887.2	1706.3	147.9	5.9
	SD	13993.8	4699.4	1836.5	4240.8	157.8	651.5	29.2	2.3
Kolmogorov- Smirnov test for normality	K-S d	0.18	0.15	0.10	0.11	0.12	0.19	0.16	0.13
	p-value	0.45	0.64	1.00	0.95	0.91	0.38	0.57	0.81
Kruskal-Wallis H-test	Chi-Square	15.4	15.6	3.4	6.2	18	1.1	17	15.7
	p-value	<0.001*	<0.001*	0.18	0.04*	<0.001*	0.6	<0.001*	<0.001*
Sediment sample 1		31428.5	17131.3	15157.2	31730.0	827.8	1666.0	99.5	8.2
Sediment sample 2		36785.5	21121.2	14654.5	28985.0	733.4	1745.5	104.2	7.0
Sediment sample 3		36785.5	19484.8	14883.8	26925.0	750.0	1785.3	118.0	5.9
Sediment sample 4		43928.5	16646.5	15617.8	28985.0	1175.0	1685.8	104.2	5.5
Mean		37232.0	18596.0	15078.3	29156.3	871.5	1720.7	106.5	6.7

* Statistically significant at critical p-value ≤ 0.05 .

Table 2

Summary results of the forward DFA.

DFA parameters	Result
Function 1	
Eigenvalue	12.8
Wilks' lambda	0.019
Canonical correlation	0.96
Function 2	
Eigen value	2.6
Wilks' lambda	0.27
Canonical correlation	0.85
Sediment source samples classified correctly (%)	
Channel banks	100.0
Rangeland surface soils	100.0
Quarrying	87.5
Total	95.8
Sampling sites for the sediment sources assigned by the DFA	
Channel banks	8.0
Rangeland surface soils	8.0
Quarrying	7.0
Squared Mahalanobis distance	
Channel banks × Rangeland surface soils	57.6
Channel banks × Quarrying	14.4
Rangeland surface soils × Quarrying	49.6
Squared Mahalanobis F-value	
Channel banks × Rangeland surface soils	49.3*
Channel banks × Quarrying	12.4*
Rangeland surface soils × Quarrying	42.4*

* Statistically significant at critical $p \leq 0.01$.

Table 3

Final results of the stepwise forward DFA.

Tracer	Wilks' lambda	Partial lambda	Wilks'	F-remove	p-level	Tolerance
Mn	0.06	0.35		17.0	<0.001	0.90
Ni	0.04	0.52		8.2	0.003	0.84
Ca	0.04	0.53		8.0	0.003	0.82
Fe	0.04	0.56		7.0	0.006	0.74

For Peer Review

Table 4

PCCA factor coordinates of the variables and the eigenvalues of the correlation matrix.

Tracer	PC 1	PC 2	PC 3	Communalities
Ca	-0.68	-0.18	0.66	0.93
Fe	0.87	-0.31	0.04	0.86
Mg	-0.47	-0.79	-0.37	0.98
Mn	0.82	-0.29	0.36	0.88
Ni	-0.86	-0.20	0.17	0.81
TOC	0.90	-0.18	0.10	0.85
Eigenvalue	3.66	0.92	0.74	
% Total variance	61.0	15.3	12.4	
Cumulative % variance	61.0	76.3	88.7	
Mean scores of the three sediment sources				
Channel banks	-0.56 a ¹	0.81 a	-0.75 a	
Rangeland surface soils	1.30 b	-0.16 ab	-0.12 ab	
Quarrying	-0.75 a	-0.65 b	0.63 b	
ANOVA results				
F-value	90.8	6.5	5.4	
p-value	<0.0001	0.006	0.01	

¹Different lower case letters indicate that the scores are significantly different at critical $p \leq 0.05$ level, based on the Tukey HSD Post Hoc test.

Table 5

Comparison of the predicted and known relative contributions from the sediment sources to the virtual sediment mixtures using the composite signatures selected by different statistical approaches and the corresponding root mean squared error (RMSE) and mean absolute error (MAE).

Statistical approaches for selecting final composite fingerprints	Source proportions	Sediment source			RMSE	MAE
		Channel banks (%)	Rangeland surface soils (%)	Quarrying (%)		
KW-H (Tracers: Ca, Fe, Mg, Mn, Ni, TOC)	Known	33.3	33.3	33.3	0.3	0.3
	Predicted	33.2	33.8	33		
	Known	5.0	5.0	90.0	19.2	17.4
	Predicted	24.3	11.8	63.8		
Combination of KW-H and DFA (Tracers: Ca, Fe, Mn, Ni)	Known	20.0	75.0	5.0	5.5	5.1
	Predicted	15.0	72.3	12.7		
	Known	33.3	33.3	33.3	2.5	2.2
	Predicted	36.6	32.9	30.5		
Combination of KW-H and PCCA (Tracers: Ca, Mg, TOC)	Known	5.0	5.0	90.0	20.9	18.9
	Predicted	26.3	12.1	61.6		
	Known	20.0	75.0	5.0	5.1	4.8
	Predicted	16.2	71.7	12.2		
Combination of KW-H and PCCA (Tracers: Ca, Mg, TOC)	Known	33.3	33.3	33.3	2.5	2.3
	Predicted	29.9	34.4	35.7		
	Known	5.0	5.0	90.0	20.2	18.6
	Predicted	24.2	13.7	62.1		
	Known	20.0	75.0	5.0	6.8	6.1
	Predicted	17.85	67.96	14.17		

Figure captions

Figure 1. Map of the study catchment and sampling sites.

Figure 2. Scatterplot of the first and second discriminant functions calculated using backward DFA associated with selection of the final composite signature comprising Ca, Fe, Mn, and Ni.

Figure 3. (a) Scree plot output from the PCCA analysis for sediment source discrimination, (b) Projection of the cases on the PC-plane using PCCA.

Figure 4. Biplots of all pairings for the tracers selected in the three final composite signatures for discriminating and apportioning source contributions to the target sediment samples.

Figure 5. Probability density functions for the estimated mean sediment source contributions using the final composite signatures selected by (a) KW-H, (b) a combination of KW-H as step one and discriminant function analysis (DFA) as step two, and (c) a combination of KW-H as step one and principal components & classification analysis (PCCA) as step two.

Fig. 1

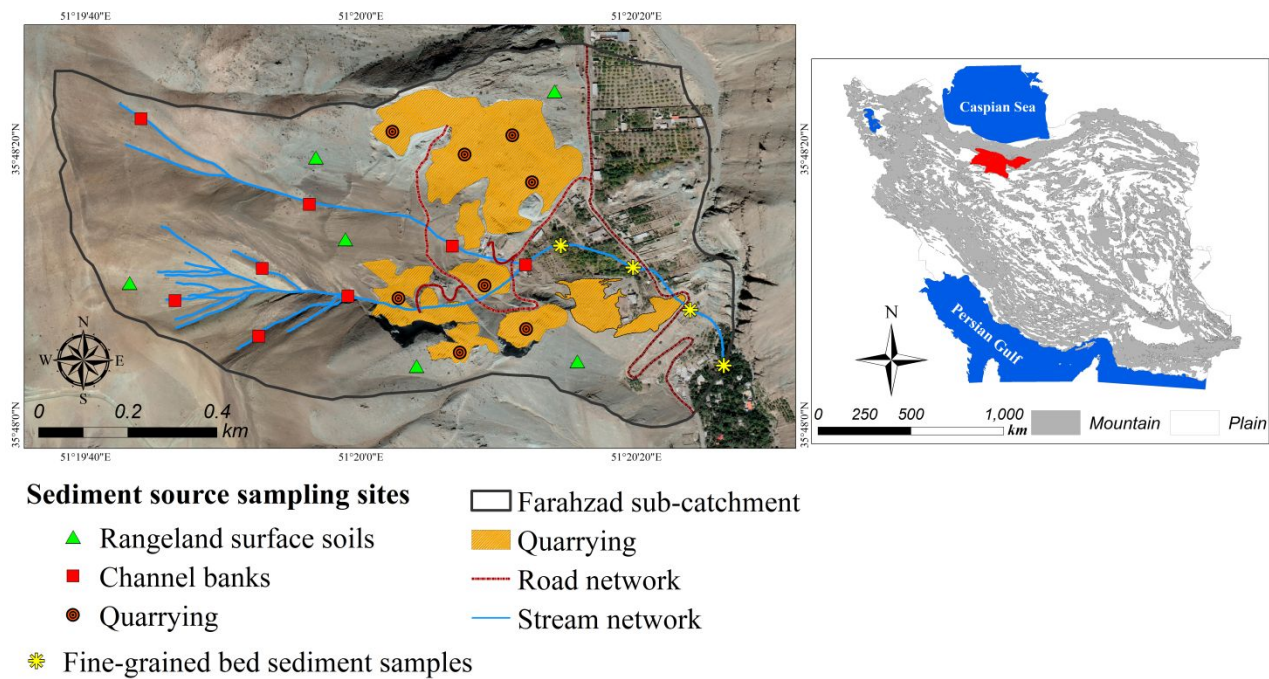


Fig. 2

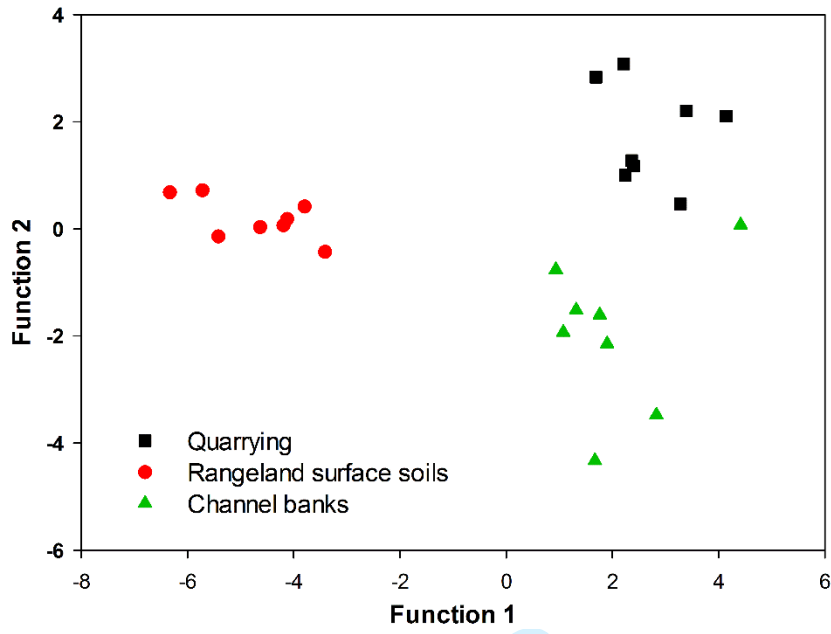


Fig. 3

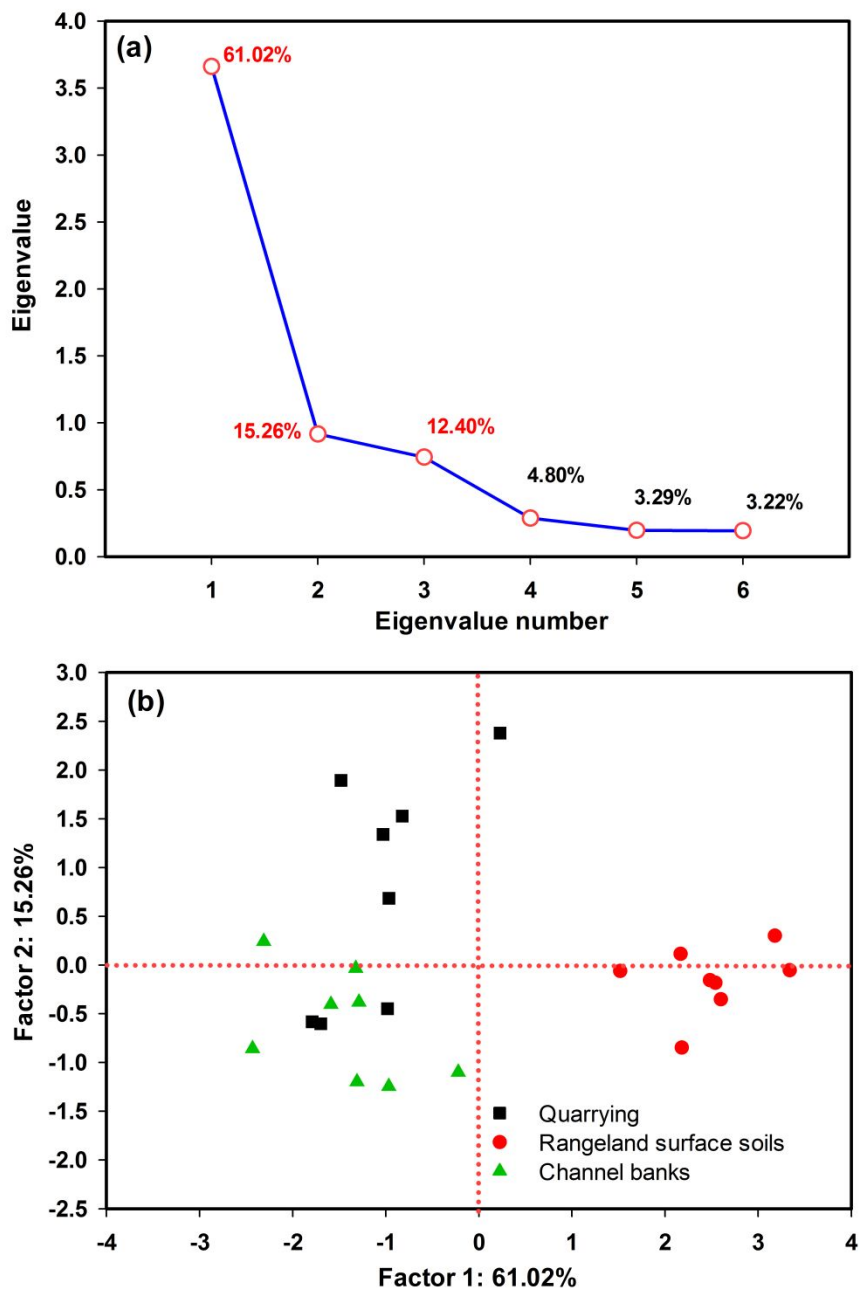


Fig. 4

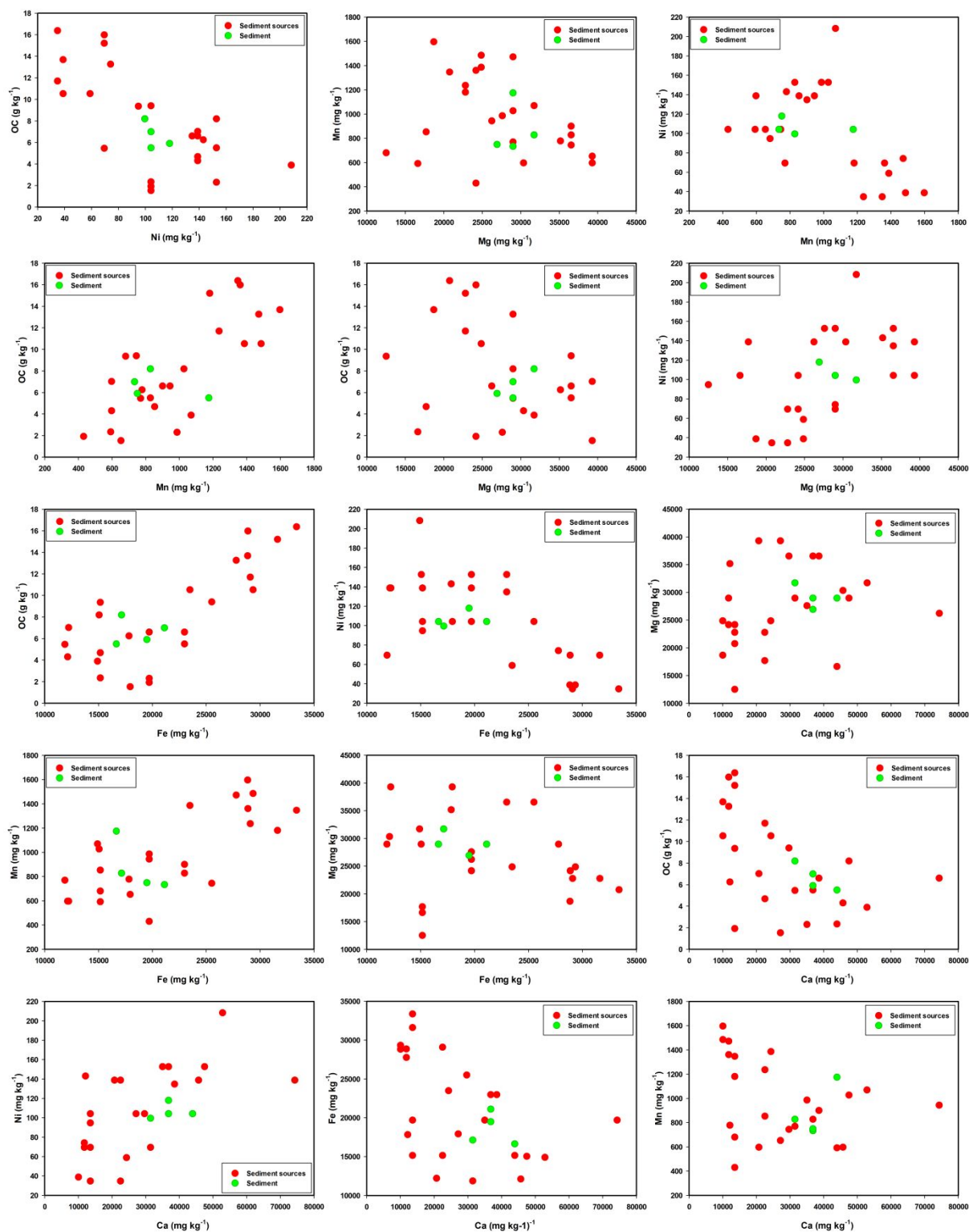
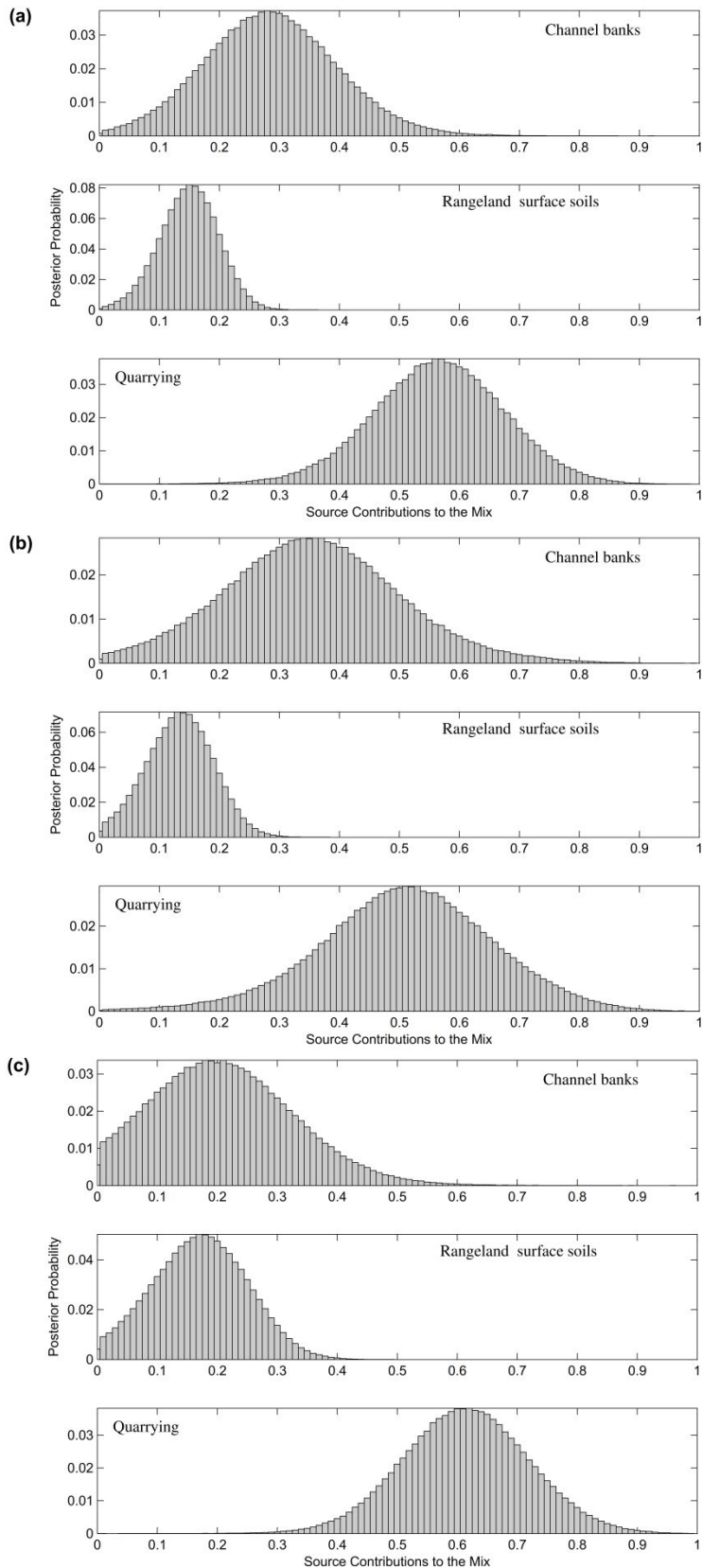


Fig. 5



view